PROCEEDINGS OF SCIENCE

Searches for CPV in D^+ decays at LHCb

S. Stracka[*†]
Università di Pisa and Sezione INFN di Pisa, Pisa, Italy
E-mail: simone.stracka@cern.ch

Singly-Cabibbo-suppressed $D^+_{(s)}$ decays are a good place to search for CP violation in charm, which in the Standard Model is expected to be small, at the level of 0.1% or less. In Cabibbo-Favored decays of charm mesons, observing a significant CP violation with the present level of precision would be a signature of new physics. We report on recent searches for CP violation in $D^+_{(s)}$ decays by the LHCb experiment, using proton-proton collision data corresponding to an integrated luminosity of 3 fb^{-1}, recorded at centre-of-mass energies of 7 and 8 TeV. In particular, we report on searches for CP violation in $D^\pm \to \eta'\pi^\pm$ and $D_s^\pm \to \eta'\pi^\pm$ decays.

VIII International Workshop On Charm Physics
5-9 September, 2016
Bologna, Italy

[*]Speaker.
[†]On behalf of the LHCb Collaboration

PoS(CHARM2016)074

1. Introduction

The charm system represents a unique probe for *CP* violation in up-type quarks. To date, no *CP* violation has been observed in the charm sector. In the Standard Model (SM), *CP* violation in mixing is expected to be small and universal, while direct *CP* violation is in general dependent on the final state [1]. Naively, direct *CP* violation in the decays of charmed mesons is also expected to be small in the SM, but sizeable enhancements (above $\mathcal{O}\left(10^{-3}\right)$) can occur both in the SM scenario - due to non-perturbative effects [2] - and in the beyond-the-SM scenario - due, e.g., to new physics contributions to the decay via penguin (loop) diagrams [3]. It is therefore interesting to investigate experimentally many decays with comparable sensitivity, to maximize the chances of observing *CP* violation, and to provide key input to the theoretical interpretation of the results in light of Standard Model or New Physics.

Charm mesons decay dominantly into hadronic final states, a large fraction of which are two-body modes. In order for non-zero *CP* asymmetries to be observable in a process, two or more interfering amplitudes with different *CP*-odd and *CP*-even phases are needed. Among two-body decays, only singly-Cabibbo-suppressed (SCS) decays can possibly involve diagrams with different weak phases (color-allowed tree-level amplitudes, and penguin and color-suppressed tree amplitudes) and thus allow *CP* violation to emerge in the SM. Even so, *CP* violation in SCS decays is expected only at the $\mathcal{O}\left(10^{-4}\right)$ to $\mathcal{O}\left(10^{-3}\right)$ level [4, 5]. No direct *CP* violation is expected in Cabibbo-favoured charm decays, which are mediated by a single weak amplitude.

There are eight singly-Cabibbo-suppressed decays of $D^{\pm}$ and $D_s^{\pm}$ mesons to two light pseudoscalar mesons. The study of these decays, taken as a whole, allows to test flavour-topology and SU(3) predictions, constrain amplitudes through triangle relations or shed light on sources of SU(3) flavour symmetry breaking. The LHCb collaboration has recently reported *CP* violation measurements for the $D^+ \to K^+\overline{K}^0$ and $D_s^+ \to K^+K^0$ decays [6, 7], which have shown no evidence for *CP* violation. However, all other $D \to PP$ decays are difficult to study experimentally at a hadronic machine, due to the presence of a neutral meson (π^0, η, η') in the final state, and have thus far only been studied in e^+e^- collisions.

In these Proceedings, the first analysis of $D_s^{\pm} \to \eta'\pi^{\pm}$ and $D^{\pm} \to \eta'\pi^{\pm}$ decays at a hadron collider is presented [8]. The most recent studies of these decays at the Belle and CLEO experiments yielded a *CP* asymmetry of $(-0.12 \pm 1.12 \pm 0.17)\%$ [9] for the singly-Cabibbo-suppressed $D^{\pm} \to \eta'\pi^{\pm}$ decay and $(-2.2 \pm 2.2 \pm 0.6)\%$ [10] for the Cabibbo-favoured $D_s^{\pm} \to \eta'\pi^{\pm}$ decay. In the LHCb experiment, the large charm production cross-sections at the LHC for pp collisions at $\sqrt{s} = 7\,\text{TeV}$ and $\sqrt{s} = 8\,\text{TeV}$ allows to take advantage of the world's largest sample of decays of charmed hadrons to mitigate the disadvantages of a hadronic environment compared to the cleaner e^+e^- collisions, and yield the most precise measurement of *CP* asymmetries in these decays to date.

2. Reconstruction and sample composition

The LHCb detector is a forward-arm spectrometer, with pseudo-rapidity coverage in the range $2 < \eta < 5$, specifically designed for high precision measurements of decays of b and c hadrons produced in pp collisions at the LHC.

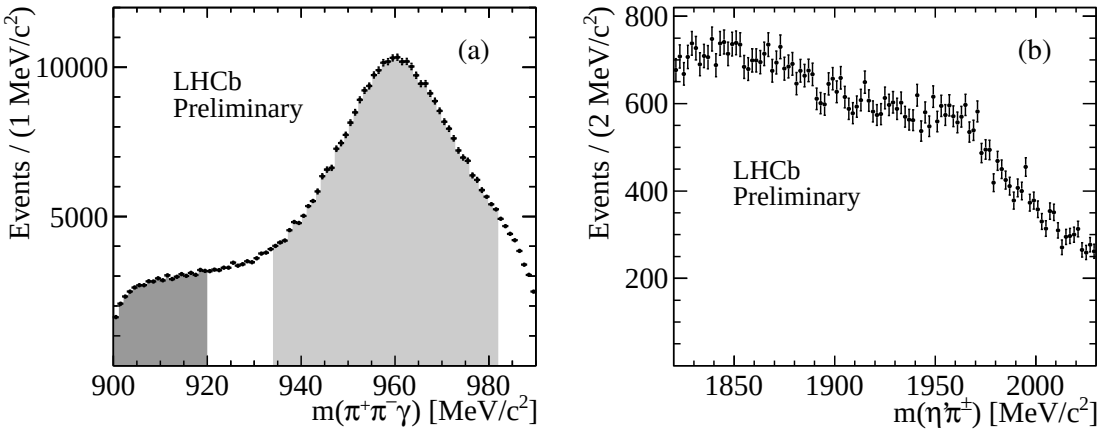

Figure 1: (a) $m(\pi^+\pi^-\gamma)$ distribution for $D^\pm_{(s)} \to \eta'\pi^\pm$ candidates. The light shaded area represents the signal region, while the dark shaded area represents the $m(\pi^+\pi^-\gamma)$ sideband. (b) $m(\eta'\pi^\pm)$ distribution for $D^\pm_{(s)} \to \eta'\pi^\pm$ candidates in the $m(\pi^+\pi^-\gamma)$ sideband.

Dealing with charm decays with neutrals in the final state poses some challenges in the hadronic environment of LHCb. The main difficulties are associated to the trigger, which relies on high-p_T displaced charged tracks, and to the high background levels. Some of the possible decay modes of the π^0, η, and η' mesons - such as $\eta' \to \pi^+\pi^-\gamma$, $\eta \to \pi^+\pi^-\gamma$, $\pi^0 \to e^+e^-\gamma$ - display a topology that allows to overcome these difficulties, by leveraging on the large production cross-section, large boost of charm mesons and good time resolution. In these decays, the displaced-track trigger can be activated by the charged particles from the η' decay, while the good D decay-vertex reconstruction can be used to suppress background. The large number of charm mesons produced in acceptance makes up for the branching fraction of the neutral meson decay into a charged mode, which may be suppressed.

The signal $D^\pm_{(s)} \to \eta'\pi^\pm$ candidates are reconstructed through the intermediate resonance decay $\eta' \to \pi^+\pi^-\gamma$, which occurs with a branching fraction $\mathscr{B} = (29.1 \pm 0.5)\%$. The η' candidates are then combined with a third displaced charged hadron (bachelor) to form a $D_{(s)}$ candidate. The $D^\pm_{(s)}$ mass is calculated by constraining the η' candidate mass to its known value, thus improving the $m(\eta'\pi)$ resolution.

The dominant backgrond contribution is combinatorial, and is studied in the $m(\pi^+\pi^-\gamma)$ sideband, shown in Fig. 1 (b). Specific background sources, such as $D^\pm_{(s)} \to X\ell^\pm\nu$ and $D^\pm_{(s)} \to XK^\pm$ decays, with $X = \eta'$, ϕ, or K^0_S, are suppressed by particle identification requirements. The main peaking background contribution originates from partially reconstructed $D^\pm_{(s)} \to \phi\pi^\pm$ decays, with $\phi \to \pi^+\pi^-\pi^0$.

3. Method

The *CP* asymmetries A_{CP} are determined from the measured (raw) asymmetries

$$A_{\rm raw}(D^\pm_{(s)} \to f^\pm) = \frac{N(D^+_{(s)} \to f^+) - N(D^-_{(s)} \to f^-)}{N(D^+_{(s)} \to f^+) + N(D^-_{(s)} \to f^-)}, \tag{3.1}$$

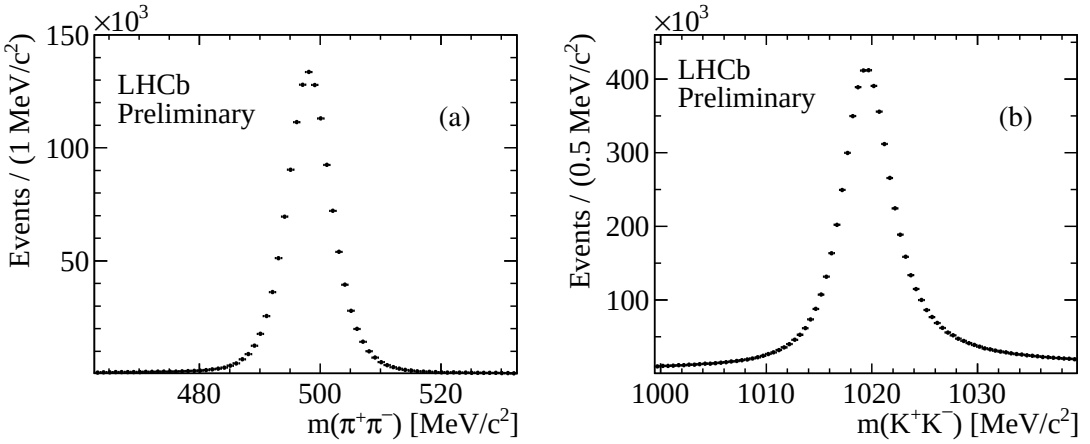

Figure 2: Distributions in $m(\pi^+\pi^-)$ for $D^\pm \to K^0_S\pi^\pm$ candidates (1.165×10^6 candidates, left) and $m(K^+K^-)$ for $D_s^\pm \to \phi\pi^\pm$ candidates (6.657×10^6 candidates, right).

where N denotes the observed yield for the decay to a given charged final state $f^\pm$.

The measured asymmetries include additional contributions other than $A_{CP}(D^\pm_{(s)} \to f^\pm)$. For small asymmetries, it is possible to approximate to first order

$$A_{\rm raw} \approx A_{CP} + A_{\rm prod} + A_{\rm det}, \tag{3.2}$$

where $A_{\rm prod}$ is the asymmetry in the production of $D^\pm_{(s)}$ mesons in high-energy pp collisions in the forward region, and $A_{\rm det}$ arises from the difference in detection efficiencies between positively and negatively charged hadrons.

These effects are studied using control decay modes for which A_{CP} is known precisely. The control decays, which have similar production and decay topologies as signal, are the Cabibbo-favoured $D^\pm \to K^0_S\pi^\pm$ and $D_s^\pm \to \phi\pi^\pm$ decays for $D^\pm \to \eta'\pi^\pm$ and $D_s^\pm \to \eta'\pi^\pm$, respectively. The CP asymmetries in these decays have been measured at the 10^{-3} level by the Belle and D0 collaborations.

The differences between the CP asymmetries measured in the $D^\pm_{(s)} \to \eta'\pi^\pm$ decays and in the corresponding control channels are defined as

$$\Delta A_{CP}(D^\pm \to \eta'\pi^\pm) = A_{\rm raw}(D^\pm \to \eta'\pi^\pm) - A_{\rm raw}(D^\pm \to K^0_S\pi^\pm) + A(\overline{K}^0 - K^0), \tag{3.3}$$

$$\Delta A_{CP}(D_s^\pm \to \eta'\pi^\pm) = A_{\rm raw}(D_s^\pm \to \eta'\pi^\pm) - A_{\rm raw}(D_s^\pm \to \phi\pi^\pm). \tag{3.4}$$

These equations assume that the kinematic distributions of the pion and of the $D_{(s)}$ meson are similar in the signal and control channels, so that detection and production asymmetries largely cancel in the difference. Equation 3.3 includes a kaon asymmetry term $A(\overline{K}^0 - K^0)$, which arises from regeneration and from mixing and CP violation in the $\overline{K}^0 - K^0$ system in $D^\pm \to K^0_S\pi^\pm$ decays. This contribution is estimated using simulations, as described in Ref. [11], to be $(-0.08 \pm 0.01)\%$.

4. Determination of the asymmetries

In order to improve the cancellation of detector asymmetries, the bachelor pion selection for signal and control sample are equalized as much as possible. The hardware trigger selections do

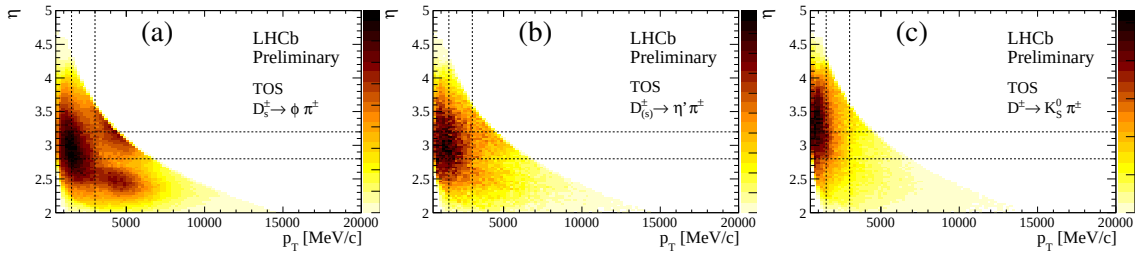

Figure 3: Distribution in $\eta - p_T$ of the bachelor pion for (a) $D_s^\pm \to \phi\pi^\pm$, (b) $D_{(s)}^\pm \to \eta'\pi^\pm$, and (c) $D^\pm \to K_S^0\pi^\pm$. The $\eta - p_T$ bin edges are marked by dashed lines.

not rely on information associated to the same-charge pion from the $D_{(s)}$ decay (the bachelor pion). Fiducial requirements are imposed to exclude kinematic regions where reconstruction and particle identification of the bachelor pion suffer from large charge-dependent asymmetries.

The data are divided into mutually exclusive subsamples, according to the two pp centre-of-mass energies and the hardware trigger selections. The data were taken with a regular swap of the polarity of the spectrometer dipole magnet. The $A_{\rm raw}$ measurements are performed separately for the two field polarities and then averaged. This can compensate for residual left-right detector asymmetries.

Since detection asymmetries depend on the kinematic properties of the process under study, $D_{(s)}^\pm$ candidates in each subsample are divided into 3×3 bins of transverse momentum and pseudorapidity of the bachelor pion. While the bachelor-pion kinematic distributions for the signal and $D_s^\pm \to \phi\pi^\pm$ control decays are in good agreement, the average bachelor-pion p_T (η) is 30% lower (5% higher) in the $D^\pm \to K_S^0\pi^\pm$ control channel (Fig. 3). The binning reduces the effect of the discrepancies between the bachelor-pion kinematic distributions for signal and control decays, thus improving the suppression of $A_{\rm det}$ in the differences of raw asymmetries.

For each subsample, the raw CP asymmetries of the $D_{(s)}^\pm \to \eta'\pi^\pm$ signal channels are determined with a maximum likelihood fit to the unbinned $\eta'\pi$ invariant mass distribution, performed simultaneously for positively and negatively charged $D_{(s)}^\pm$ candidates, and for the nine $p_T - \eta$ bins. Due to the high purity of the control samples, the raw CP asymmetries for the $D_s^\pm \to \phi\pi^\pm$ and $D^\pm \to K_S^0\pi^\pm$ decay modes are extracted by sideband subtraction. For each subsample, the differences of raw asymmetries for signal and associated control channels are calculated in each bin. Weighted averages of the results obtained in the nine $p_T - \eta$ bins are then evaluated.

The model for the fit to the $m(\eta'\pi)$ distribution comprises two signal components for the $D_{(s)}^\pm$ resonances, a combinatorial background component, and two peaking components accounting for background from $D_{(s)}^\pm \to \phi_{3\pi}\pi^\pm$ decays. The results of the fit are shown in Fig. 4. The extracted yields for the $D^\pm \to \eta'\pi^\pm$ and $D_s^\pm \to \eta'\pi^\pm$ components, combined over all kinematic bins, pp centre-of-mass energies, and hardware trigger selections, are $N(D^\pm \to \eta'\pi^\pm) = (62.7\pm0.4)\times10^3$ and $N(D_s^\pm \to \eta'\pi^\pm) = (152.2\pm0.5)\times10^3$, respectively. An average charge asymmetry of $(0.92\pm 0.72)\%$ is observed in the combinatorial background.

The contributions to the systematic uncertainty on the inverse-variance weighted ΔA_{CP} average are summarized in Table 1. The overall systematic uncertainties are obtained by adding the individual contributions in quadrature.

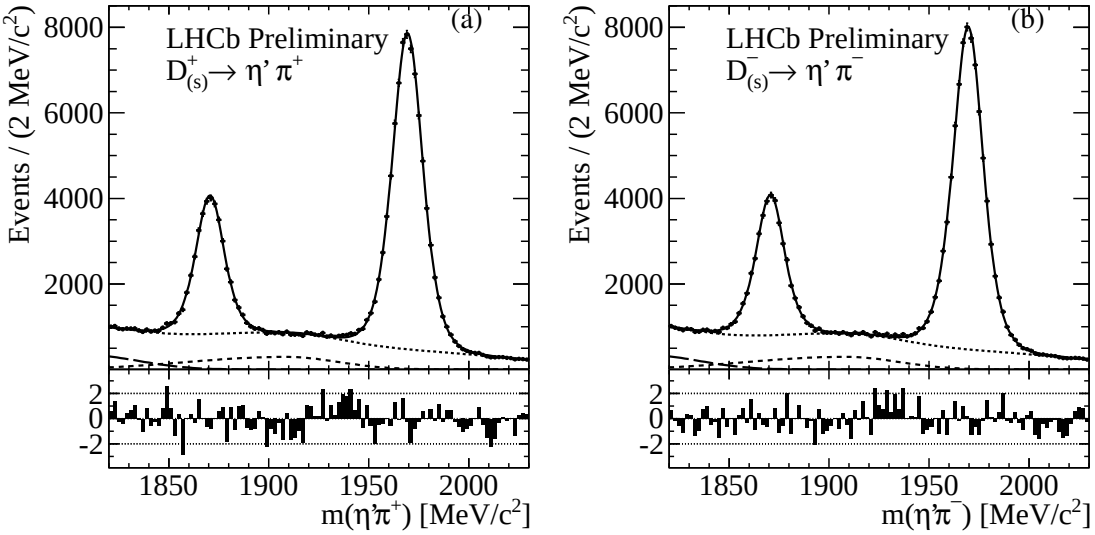

Figure 4: $\eta'\pi^\pm$ mass distribution, combined over all kinematic bins, pp centre-of-mass energies, and hardware trigger selections, for (a) positively and (b) negatively charged $D^\pm_{(s)}$ candidates. Points with errors represent data, while the curves represent the fitted model (solid), the $D^\pm_s \to \phi_{3\pi}\pi^\pm$ (dashed) and $D^\pm \to \phi_{3\pi}\pi^\pm$ (long-dashed) components, and the sum of all background contributions (dotted), including combinatorial background. Residuals divided by the corresponding uncertainty are shown under each plot.

The dominant source of systematic uncertainty is background parameterization. Several different parameterizations are used for the background component: a fourth-order polynomial, a second-order polynomial, a concave empiric function. The peaking background contributions are also varied. A systematic uncertainty is assigned based on the observed discrepancies between measurements relying on different parameterizations.

Sources of systematic uncertainty associated to the $D_{(s)}$ production mechanisms are instead found to be small. These include the contribution to the signal yield from $D^\pm_s$ mesons originating from the decay of a b hadron, or the dependence of $D_{(s)}$ production asymmetry on p_T and η of the charm meson.

Source	$\delta[\Delta A_{CP}(D^\pm)]$	$\delta[\Delta A_{CP}(D^\pm_s)]$
Non-prompt charm	0.03	0.03
Trigger	0.09	0.09
Background model	0.50	0.19
Fit procedure	0.16	0.09
Sideband subtraction	0.03	0.02
K^0 asymmetry	0.08	–
$D^\pm_{(s)}$ production asymmetry	0.07	0.02
Total	0.55	0.24

Table 1: Systematic uncertainties (absolute values in %) on ΔA_{CP}. The total systematic uncertainty is the sum in quadrature of the individual contributions.

5. Results and summary

Using pp collision data collected by the LHCb experiment at centre-of-mass energies of 7 and 8 TeV, the differences in *CP* asymmetries between $D^\pm \to \eta'\pi^\pm$ and $D^\pm \to K^0_S\pi^\pm$ decays, and between $D^\pm_s \to \eta'\pi^\pm$ and $D^\pm_s \to \phi\pi^\pm$ decays, are measured to be

$$\Delta A_{CP}(D^\pm \to \eta'\pi^\pm) = (-0.58 \pm 0.72 \pm 0.55)\% \text{ and}$$
$$\Delta A_{CP}(D^\pm_s \to \eta'\pi^\pm) = (-0.44 \pm 0.36 \pm 0.24)\%.$$

In all cases, the first uncertainties are statistical and the second are systematic.

Using the previously measured values of the *CP* asymmetries in control decays, $A_{CP}(D^\pm \to K^0_S\pi^\pm) = (-0.024 \pm 0.094 \pm 0.067)\%$ [12] and $A_{CP}(D^\pm_s \to \phi\pi^\pm) = (-0.38 \pm 0.26 \pm 0.08)\%$ [13], the individual *CP* asymmetries are found to be

$$A_{CP}(D^\pm \to \eta'\pi^\pm) = (-0.61 \pm 0.72 \pm 0.55 \pm 0.12)\% \text{ and}$$
$$A_{CP}(D^\pm_s \to \eta'\pi^\pm) = (-0.82 \pm 0.36 \pm 0.24 \pm 0.27)\%,$$

where the last contribution to the uncertainty is the uncertainty on the $A_{CP}(D^\pm \to K^0_S\pi^\pm)$ and $A_{CP}(D^\pm_s \to \phi\pi^\pm)$ measurements.

The measured values show no evidence of *CP* violation, and are consistent with SM expectations [4, 5] and with previous results obtained in e^+e^- collisions [9, 10]. They are the most precise measurements of *CP* asymmetries in the $D^\pm \to \eta'\pi^\pm$ and $D^\pm_s \to \eta'\pi^\pm$ decays to date [8]. The analysis of charged decay modes of other neutral mesons (π^0, η) may allow other measurements of *CP* asymmetries in $D^\pm$ and $D^\pm_s$ decays, previously unanticipated at a hadron collider experiment.

References

[1] I. I. Bigi, A. Paul, and S. Recksiegel, *JHEP* **06** (2011) 089 [arXiv:1103.5785].

[2] M. Golden and B. Grinstein, *Phys. Lett.* **B222** (1989) 501.

[3] Y. Grossman, A. Kagan, and Y. Nir, *Phys. Rev.* **D75** (2007) 036008 [arXiv:hep-ph/0609178].

[4] H.-Y. Cheng, and C.-W. Chiang, *Phys. Rev.* **D85** (2012) 034036 [arXiv:1201.0785].

[5] H.-n. Li, C.-D. Lu, and F.-S. Yu, *Phys. Rev.* **D86** (2012) 036012 [arXiv:1203.3120].

[6] LHCb collaboration, R. Aaij *et al.*, *JHEP* **10** (2014) 025 [arXiv:1406.2624].

[7] LHCb collaboration, R. Aaij *et al.*, *JHEP* **06** (2013) 112 [arXiv:1303.4906].

[8] LHCb collaboration, R. Aaij *et al.*, LHCb-PAPER-2016-041, in preparation.

[9] Belle collaboration, E. Won *et al.*, *Phys. Rev. Lett.* **107** (2011) 221801 [arXiv:1107.0553].

[10] CLEO collaboration, P. U. E. Onyisi *et al.*, *Phys. Rev.* **D88** (2013) 032009 [arXiv:1306.5363].

[11] LHCb collaboration, R. Aaij *et al.*, *JHEP* **07** (2014) 041 [arXiv:1405.2797].

[12] Belle collaboration, B. R. Ko *et al.*, *Phys. Rev. Lett.* **109** (2012) 021601 [arXiv:1203.6409].

[13] D0 collaboration, V. M. Abazov *et al.*, *Phys. Rev. Lett.* **112** (2014) 111804 [arXiv:1312.0741].